

Compact steep-spectrum sources from the S4 sample

D.J. Saikia¹, S. Jeyakumar¹ C.J. Salter², P. Thomasson³, R.E. Spencer³
and F. Mantovani⁴

¹ Tata Institute of Fundamental Research, National Centre for Radio Astrophysics, P.B. No. 3, Ganeshkhind, Pune 411 007, India

² Arecibo Observatory, HC3 Box 53995, Arecibo, Puerto Rico 00612, USA

³ University of Manchester, NRAL, Jodrell Bank, Macclesfield, Cheshire, SK11 9DL, UK

⁴ Istituto di Radioastronomia del CNR, Via P. Gobetti 101, I-40129 Bologna, Italy

Received:

ABSTRACT

We present the results of 5-GHz observations with the VLA A-array of a sample of candidate Compact Steep Spectrum sources (CSSs) selected from the S4 survey. We also estimate the symmetry parameters of high-luminosity CSSs selected from different samples of radio sources, and compare these with the larger sources of similar luminosity to understand their evolution and the consistency of the CSSs with the unified scheme for radio galaxies and quasars. The majority of CSSs are likely to be young sources advancing outwards through a dense asymmetric environment. The radio properties of CSSs are found to be consistent with the unified scheme, in which the axes of the quasars are observed close to the line of sight, while radio galaxies are observed close to the plane of the sky.

Key words: galaxies: active - galaxies: jets - galaxies: nuclei - quasars: general - radio continuum: galaxies

1 INTRODUCTION

High-resolution radio observations of compact steep-spectrum sources (CSSs) and the GHz-peaked spectrum (GPS) sources (cf. Fanti et al. 1990; Sanghera et al. 1995 and references therein; Dallacasa et al. 1995, 1998; Stanghellini et al. 1997; O’Dea 1998) reveal a variety of structures reminiscent of those seen in the more extended sources. For the present study, a CSS source is defined as being less than about 20 kpc in size ($H_0 = 100 \text{ km s}^{-1} \text{ Mpc}^{-1}$ and $q_0 = 0$), and having a steep high-frequency radio spectrum ($\alpha \geq 0.5$, where $S \propto \nu^{-\alpha}$). The highly compact GPS sources, with turnover frequencies in the GHz range, are included. The majority of CSS and GPS sources have double-lobed structures, often showing nuclear or core components. The GPS sources have been proposed to be miniature versions of the classical Fanaroff-Riley class II sources, and have been proposed to evolve from a GPS to a CSS and then on to a larger FRII source (cf. Carvalho 1985; Mutel & Phillips 1988; Fanti et al. 1995; Begelman 1996; Readhead et al. 1996a,b; Owsianik & Conway 1998; de Vries et al. 1998).

The detection of radio cores in a large number of the GPS and CSS sources has made it possible to estimate the symmetry parameters of this class of objects reliably, and permits the probing of their environment on these scales. Testing of the consistency of the CSSs with the expectations of the unification scheme (Scheuer 1987; Barthel 1989;

Antonucci 1993; Urry & Padovani 1995) for radio galaxies and quasars is also possible. In an earlier study, Saikia et al. (1995, hereinafter referred to as S95) found CSSs to be more asymmetric than the larger sources suggesting that their jets on these scales are propagating outwards through an asymmetric environment. They also reported that the core strengths and symmetry parameters of CSSs were consistent with the unified scheme.

In this paper, we first present radio observations with the Very Large Array (VLA) of a sample of CSSs selected from the S4 survey at 5 GHz (Pauliny-Toth et al. 1978), and which were earlier found to be unresolved or partially resolved with the Westerbork telescope at 5 GHz (Kapahi 1981). We then re-examine the trends reported in S95 using the S4 sample, as well as more recent information on the detection of radio cores in the samples considered by S95. The radio observations are presented in Section 2, while in Section 3 we describe the sample of sources used in our estimates of the symmetry parameters. In Section 4, we examine the dependence of the symmetry parameters on linear size, optical identification and core strength, with emphasis on studying the evolution and consistency with the unified scheme of CSSs. The results are summarized in Section 5.

2 THE S4 SAMPLE OF RADIO SOURCES

Complete samples of radio sources provide a powerful means of studying the properties and evolution of radio sources with age and cosmic epoch, as well as selecting individual sources for detailed studies of the physical processes responsible for their energetics and structure. However, only a few complete samples of radio sources have reasonably satisfactory information on the optical identification of the host galaxies and measurements of their redshifts. These include the 3CR (Laing, Riley & Longair 1983) and MRC (Large et al. 1981; Kapahi et al. 1998a, b) samples selected at low radio frequencies, the 2-Jy all-sky survey at 2.7 GHz (Wall & Peacock 1985, and references therein), the PKS 100-mJy deep survey (Dunlop et al. 1989) and the S4 survey (Pauliny-Toth et al. 1978; Stickel & Kühr 1994). The S4 survey is complete to 0.5 Jy at 5 GHz and lies intermediate in brightness between the Wall & Peacock (1985) and the Dunlop et al. (1989) surveys. It covers the region between $+35^\circ \leq \delta \leq +70^\circ$ and consists of 270 sources with $|b^{II}| \geq 10^\circ$. This complete sample, with updates of the optical identifications and redshifts, has been presented by Stickel & Kühr (1994).

2.1 Radio observations

A sample of 42 candidate CSSs from the S4 survey with a flux density at 5 GHz ≥ 0.5 Jy, and which were either unresolved or partially resolved with the WSRT at 5 GHz, were observed with the VLA A-array at 4835 MHz on 1985 February 10. The radio source 0625+50 with $S(5\text{ GHz}) = 0.493$ Jy (Pauliny-Toth et al. 1978) was also observed. Each source was observed in the snapshot mode for about 5-10 min. The data were calibrated at the VLA and reduced using AIPS. All flux densities are on the Baars et al. (1977) scale.

The results of the VLA observations are presented as radio images in Figure 1 for all the well-resolved objects, except 0707+68, 1244+49, 1402+66 and 2323+43, which were presented in Sanghera et al. (1995), and the well-known 3CR sources 0809+48 (3C196) and 0906+43 (3C216) whose images are available in the literature. Some of the observational parameters are summarized in Table 1, which is arranged as follows. Column 1: source name in the IAU format; column 2: optical identification where G denotes a galaxy, Q a quasar and EF an empty field; column 3: the major and minor axes of the restoring beam in arcsec, and its position angle in deg; column 4: the rms noise in the total-intensity images in units of mJy/beam; columns 5 and 6: the core and total flux density in the images. The core flux density is the peak brightness of this feature in units of mJy/beam, while the total flux density in units of mJy has been estimated by specifying a box around the radio source.

2.2 Notes on sources

0223+34: There is evidence of weak emission to the east of the core, which was noted by Spencer et al. (1989) but not confirmed by Dallacasa et al. (1995). VLBI observations show a bright compact component and a weaker one separated by about 0."5 (Dallacasa et al. 1995).

0655+69: This is a triple source (Patnaik et al. 1992). Ev-

Table 1. Observed properties of the sources

Source	Opt	Beam size			σ	S_c	S_{tot}
		maj.	min.	PA			
(1)	(2)	(3)	(4)	(5)	(6)		
0011+34	EF	0.51	0.37	150	0.06		395
0223+34	Q	0.47	0.36	150	0.13		1638
0307+44	Q	0.48	0.34	151	0.06	190	600
0420+34	EF	0.47	0.37	152	0.06	257	476
0625+50		0.51	0.34	1	0.06		430
0639+59	EF	0.54	0.35	8	0.10		526
0655+69	EF	0.60	0.35	10	0.08		689
0657+68	G	0.56	0.33	9	0.10	59	499
0659+44	EF	0.48	0.34	6	0.07		560
0703+46	Q	0.44	0.33	7	0.06		594
0707+68	Q	0.58	0.35	5	0.11		745
0809+48	Q	0.48	0.34	5	0.33		3967
0827+37	Q	0.46	0.35	177	0.11		847
0840+42	EF	0.48	0.35	0	0.05		554
0902+49	Q	0.50	0.34	8	0.05	401	466
0906+43	Q	0.49	0.34	6	0.11	871	1570
0945+66	G	0.53	0.37	13	0.10		1215
1014+39	G	0.44	0.37	10	0.06		487
1020+59	Q	0.47	0.37	14	0.05	22	484
1128+45	Q	0.46	0.37	37	0.06		656
1131+43	G	0.45	0.37	39	0.04		500
1133+43	EF	0.45	0.37	30	0.05		505
1138+59	EF	0.49	0.36	30	0.05		772
1153+59	G	0.50	0.33	12	0.09	80	416
1156+54	EF	0.51	0.34	10	0.08		625
1225+36	Q	0.50	0.36	10	0.07		783
1242+41	Q	0.49	0.36	3	0.07		690
1244+49	G	0.48	0.33	4	0.05	40	573
1402+66	EF	0.55	0.33	11	0.07		721
1409+52	G	0.50	0.34	11	0.36		6438
1413+34	EF	0.46	0.36	6	0.08		930
1818+35	Q	0.75	0.48	72	0.17	53	474
1819+39	G	0.74	0.40	89	0.49		953
1843+40	G	0.74	0.40	86	0.32		567
1943+54	G	0.64	0.36	109	0.15		885
2015+65	Q	0.68	0.34	112	0.17		575
2207+37	Q	0.51	0.38	148	0.11		829
2255+41	Q	0.49	0.38	148	0.18		1063
2304+37	G	0.47	0.34	155	0.07		570
2311+46	Q	0.51	0.34	155	0.13	75	760
2323+43	G	0.47	0.34	156	0.08		892
2358+40	EF	0.48	0.36	153	0.10		581

idence of the diffuse emission to the east is barely seen in the high-resolution image by Patnaik et al.

0827+37: A plume of emission to the north and diffuse emission to the south are seen on the VLA $\lambda 20\text{cm}$ image of Xu et al. (1995).

0902+49: Comparison of the core flux density at $\lambda 6\text{cm}$ with those presented by Stanghellini et al. (1990) shows that this has not varied significantly over a period of about 1 yr. VLBI observations show the core to be extended (Henstock et al. 1995). It appears to have a one-sided radio structure.

0945+66: A lower-resolution $\lambda 20\text{cm}$ image by Xu et al. (1995) shows the source to be extended along a similar PA.

1014+39: A lower-resolution $\lambda 20\text{cm}$ image has been published by Machalski & Condon (1983).

1138+59: VLBI observations show two sets of components

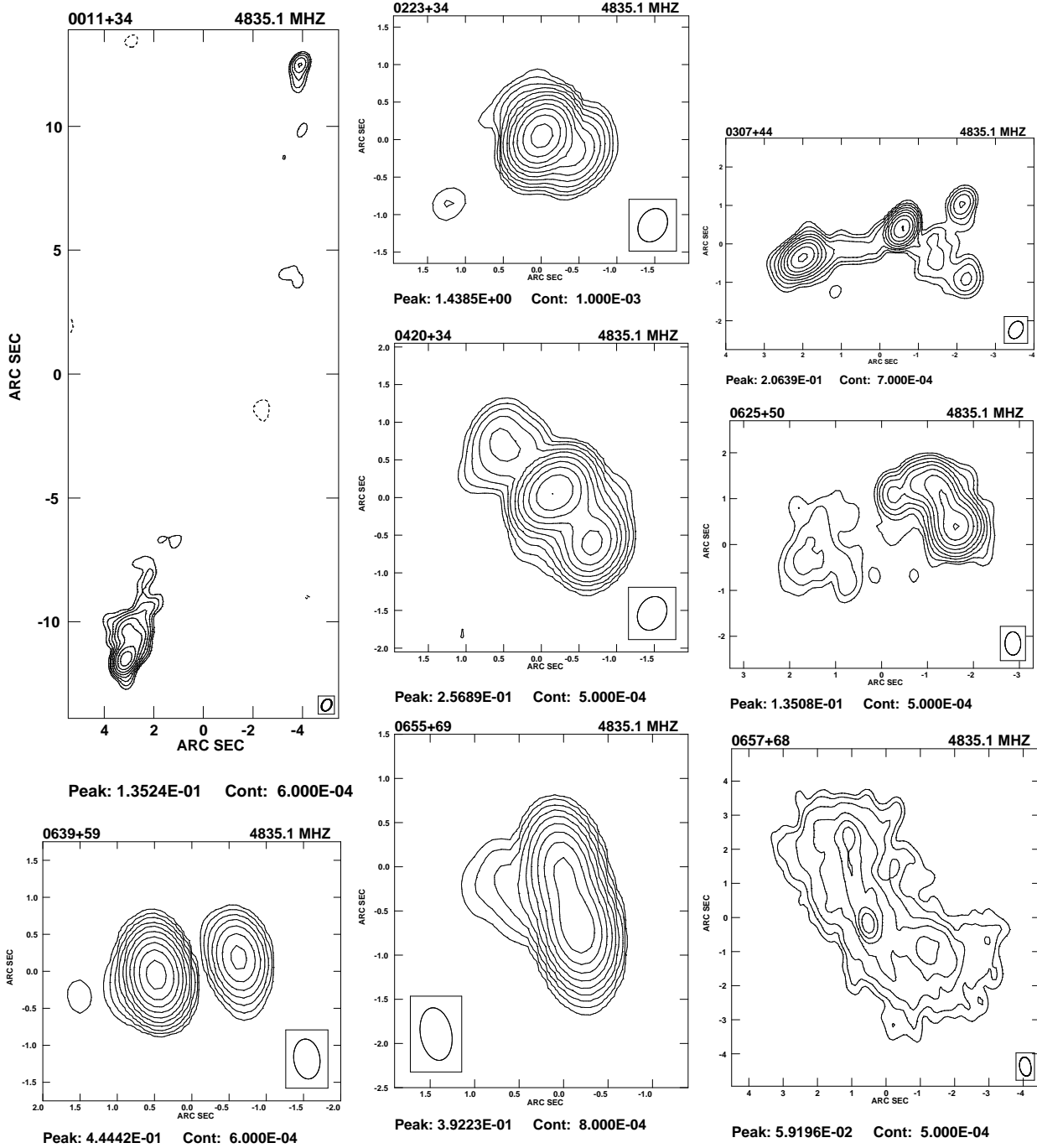


Figure 1. VLA images of our sample of S4 sources. The contour levels for all the images are $-1, 1, 2, 4, 8, 16, \dots$ times the first contour level. The peak brightness in the image and the level of the first contour in units of mJy/beam are given below the images.

with an overall separation of ~ 225 mas along a PA of $\sim 170^\circ$ (Xu et al. 1995).

1818+35: VLA observations at $\lambda 20$ and 6cm show this to be a double source, with only a single component being detected on VLBI scales (Taylor et al. 1996).

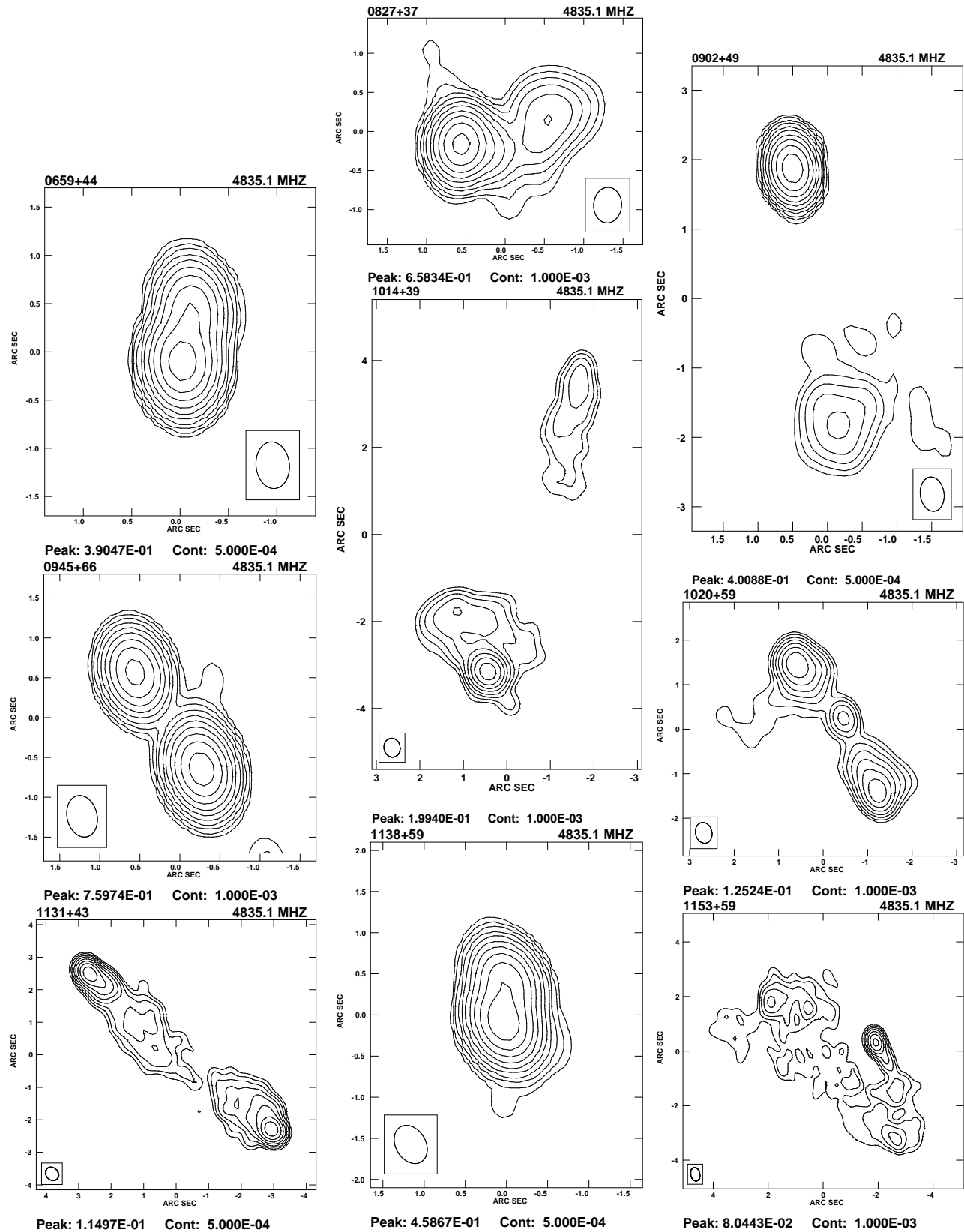
2207+37: VLBI observations show a strongly curved jet-like structure towards the west (Thakkar et al. 1995; Xu et al. 1995).

2311+46: The VLBI image has a prominent component with an extension, and has been modelled to consist of three

components with an overall separation of ~ 1.7 mas (Xu et al. 1995).

3 SAMPLE OF SOURCES AND THEIR SYMMETRY PARAMETERS

We note that although we use 20 kpc as a working definition for the upper limit to the size of a CSS, any adopted value will be somewhat ad hoc. The detailed structure of a source



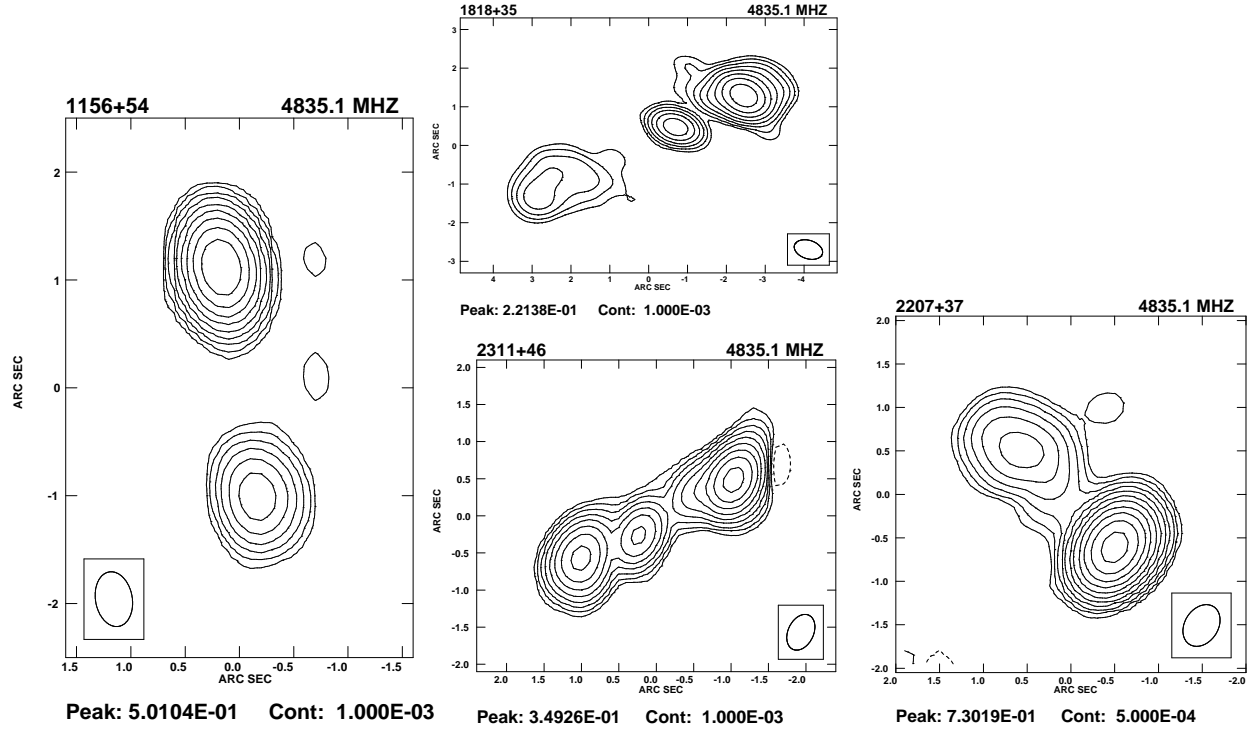


Table 2. Symmetry parameters of sample of sources

IAU	Alt.	Id	z	size	f_c	Δ	r_D	r_L
0107+315	3C34	G	0.689	222	0.00088	2.8	1.03	1.3
0125+287	3C42	G	0.395	102	0.0033	7	1.07	1.25
0307+444	4C+44.07	Q	1.165	24.6	0.14	5.5	1.65	5.5
0428+205	OF247	G	0.219	0.51	0.12	4.5	4.69	0.16
0707+689	4C+68.08	Q	1.139	6.7	0.059	7	1.24	2.15
0725+147	3C181	Q	1.382	36	0.009	3	2.8	1.9
0806+426	3C194	G	1.184	80	0.0060	24	1.03	0.66
1007+417	4C+41.21	Q	0.611	147	0.23	10	1.6	20.3
1030+585	3C244.1	G	0.428	193	0.0018	4.5	1.1	1.3
1108+359	3C252	G	1.105	321	0.0052	4.5	1.8	2
1213+538	4C+53.24	Q	1.065	190	0.0069	4.5	1.55	0.9
1225+368	B2	Q	1.975	0.35	0.04	10.5	1.4	14.8
1317+520	4C+52.27	Q	1.06	150	0.56	20	1.9	0.55
1358+624	4C+62.22	G	0.431	0.149	0.0091	10.5	2.92	2.26
1420+198	3C300	G	0.272	269	0.0075	4.5	2.4	0.32
1529+357	3C320	G	0.342	51	0.015	11	1.76	0.97
1547+215	3C324	G	1.206	63.5	0.0002	4	1.16	2.6
1549+628	3C325	G	0.86	83.7	0.0025	3.5	1.32	0.48
1609+660	3C330	G	0.55	263	0.00033	2.5	1.07	0.33
1627+234	3C340	G	0.775	223	0.0024	1.5	1.06	2.27
1819+396	4C+39.56	G	0.798	2.85	0.10	5.5	2.75	0.18
1829+290	4C+29.56	G	0.842	11.8	0.96	21	1.65	1.23
1939+605	3C401	G	0.201	44.8	0.027	14	1.4	1.34
1943+546	TXS	G	0.263	0.11	0.04	5	1.81	0.41
2230+114	4C+11.69	Q	1.037	14	0.98	4.6	1.7	2.25
2324+405	3C462	G	0.394	85	0.042	3	1.19	0.58
2342+821		Q	0.735	0.83	0.14	11	1.39	36.15
2356+436	3C470	G	1.653	155	0.0011	3.5	1.38	0.12

will be influenced by the external environment which could sometimes be asymmetric on significantly larger scales, as can be seen in the optical broad- and narrow-band images of many high-redshift galaxies. Bearing this in mind, we have considered the symmetry parameters for well-observed complete samples of sources and studied their variations with linear size, with particular emphasis on the CSSs. We have considered well-studied samples with a high degree of completeness in optical identifications and redshift measurements; any missing objects are unlikely to affect the trends reported in this paper. We have chosen the 3CR complete sample (Laing, Riley & Longair 1983) with a radio luminosity at 178 MHz $\geq 10^{26}$ W Hz $^{-1}$ sr $^{-1}$. A luminosity limit higher than the value for differentiating between the two Fanaroff & Riley (1974) classes was chosen to minimise the contamination by border-line objects which could be distorted Fanaroff-Riley class I objects. To improve the statistics for high-luminosity sources, we have also considered the complete sample of S4 radio sources (Kapahi 1981; Stickel & Kühr 1994) with $\alpha_{1400}^{5000} \geq 0.5$ and luminosity at 5000 MHz $\geq 5 \times 10^{24}$ W Hz $^{-1}$ sr $^{-1}$. The luminosity cutoff at 5000 MHz is similar to that at 178 MHz for a source with a spectral index of 0.8. In addition, we have considered the 3C and Peacock & Wall (1982, hereinafter referred to as PW) samples of CSSs (Spencer et al. 1989) satisfying the above luminosity cutoffs. All the sources in our sample were required to have a good candidate or confirmed radio core. This is important for a reliable estimation of the symmetry parameters, particularly for the small sources. We have also not considered the complex sources whose symmetry parameters are not easily identifiable. In this paper, we re-examine the trends reported by S95 which was based almost entirely on the high-luminosity 3CR radio sources. We note that since the appearance of S95, more radio cores have been identified in both CSSs and larger sources.

We are left with a sample of 109 sources, of which 61 are galaxies, and 48 quasars. The 4 broad-line radio galaxies in the sample have been included with the quasars. Of these 109, there are 27 CSSs, of which 13 are galaxies and 14 quasars. The sample considered by S95 consisted of 81 sources. The 28 additional sources are listed in Table 2 which is arranged as follows: Column 1: source name; column 2: an alternative name; column 3: optical identification where G denotes a galaxy and Q a quasar; column 4: redshift; column 5: the projected linear size in kpc; column 6: the fraction of the emission from the core at an emitted frequency of 8 GHz, assuming spectral indices of 0 and 1 for the nuclear and extended emission; column 7: the misalignment angle Δ which is the supplement of the angle formed at the core by the outer hot-spots; column 8: the ratio, r_D , of the separation from the nucleus of the farther component to that of the nearer one; column 9: the ratio, r_L , of the integrated flux densities of the farther and nearer components. Usually, these have been estimated from low-resolution images at about 5 GHz to minimize the effects of any missing flux density. While estimating r_D and Δ , we have used the brightest peak in each outer component. Extensions which are fainter than these by more than about a factor of 3 have been ignored.

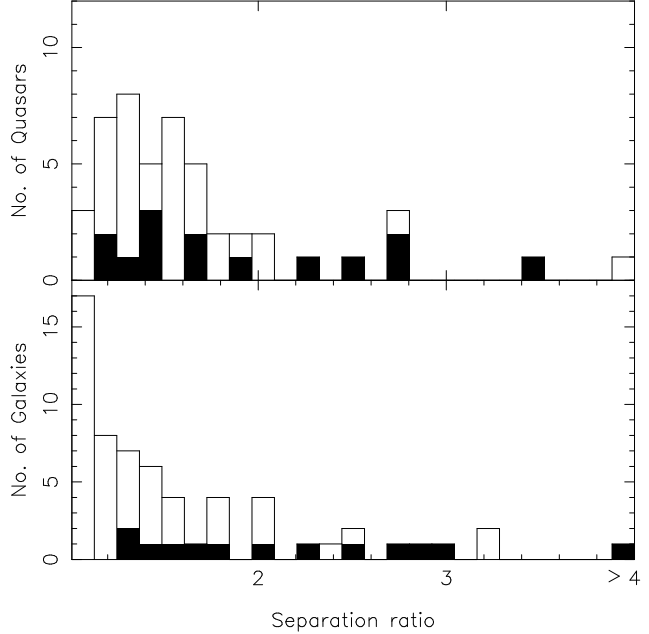


Figure 2. The distributions of the ratio, r_D , of the separations of the outer hot-spots from the nucleus, for the radio galaxies and quasars in the entire sample. The CSS sources are shown in black.

4 RELATIVISTIC MOTION AND SYMMETRY PARAMETERS

After including the results from our observations of the S4 sample, and more recent information from the literature, we have re-examined the trends reported in S95. We do not present most of the figures since the results are similar to those presented in S95, but summarise the conclusions in this section.

(i) The relative core strength for the quasars are larger than for the galaxies, consistent with the unified scheme. This is also true for the CSS subsamples, suggesting that their members are also consistent with the unified scheme. The median values of f_c are 0.07 and 0.004 for the quasars and galaxies in the entire sample, and 0.10 and 0.007 for the CSS quasars and galaxies. These values are consistent with the expectations of the unified scheme (cf. Saikia & Kulkarni 1994; Hardcastle et al. 1998).

(ii) The sources with strong cores, $f_c \geq 0.1$, which are almost all quasars, and those with small sizes tend to be more misaligned. The median value of Δ for sources with $f_c \geq 0.1$ is 11° compared to about 5.5° for the sources with weaker cores. Although this could be due to projection effects, large misalignments in a number of CSSs with weak cores suggests than interactions with the environment also play a significant role.

(iii) The distributions of the separation ratio, r_D , for the entire sample of sources is shown in Figure 2. The CSSs are shown in black. The deficit of symmetric quasars, which is attributable to orientation, is clearly seen. It is also striking that the CSSs associated with both radio galaxies and quasars have a flatter distribution with higher median values. The median value of r_D for the CSS galaxies is about

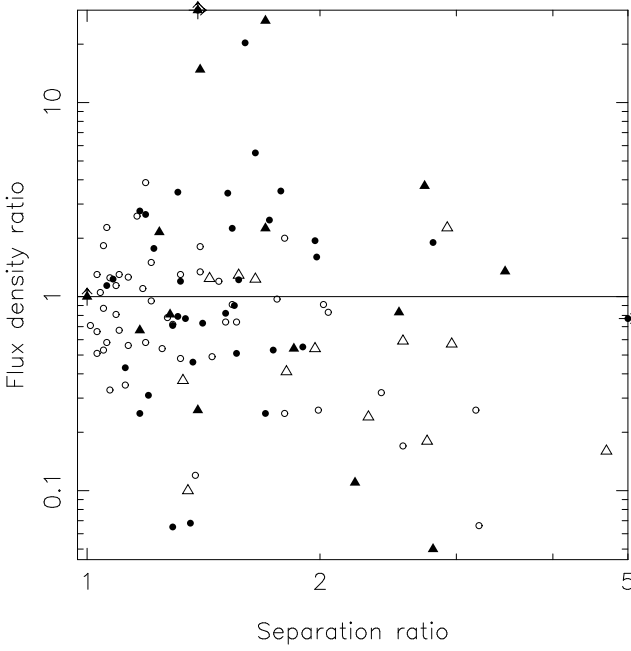


Figure 3. The log r_D - log r_L diagram for the radio galaxies and quasars. The filled and open triangles denote CSS quasars and radio galaxies, while filled and open circles denote larger-sized quasars and radio galaxies. The sources whose values lie outside the range of the box shown are marked with an arrow.

1.97 while the value for the larger galaxies is 1.33. The corresponding values for the quasars are 1.70 and 1.52. The smallest value of r_D for the CSS quasars and galaxies are about 1.17 and 1.33 respectively.

(iv) The median flux density ratio, r_L , defined to be > 1 , for the CSS quasars and galaxies are 2.99 and 2.26 respectively, compared to 1.95 and 1.51 for the larger quasars and galaxies respectively. Although these appear to be consistent with the trend expected in the unified scheme, many of the bright components are closer to the nucleus, which is not as predicted (Figure 3). This is seen in a large fraction of the CSSs, especially among those associated with galaxies where the effects of orientation are minimal, and can be understood in terms of propagation of jets through an asymmetric environment. The component on the denser side appears closer and also brighter due to higher dissipation of energy. Considering the most asymmetric objects in terms of the location of the outer components, say $r_D \geq 1.8$, 14 of the 15 galaxies have the brighter component closer compared to 6 of the 11 quasars. Numerical and analytical estimates for the propagation of jets through reasonably asymmetric environments on opposite sides of the nucleus can reproduce the observed asymmetries (Jeyakumar et al., in preparation). Evidence of such asymmetries in the distribution of gas, which might be related to the fuelling of the radio source, is sometimes provided through a huge differential rotation measure on opposite sides of the nucleus (Mantovani et al. 1994; Junor et al. 1999).

5 CONCLUDING REMARKS

The radio properties of CSSs are consistent with the unified scheme in which galaxies are seen close to the sky plane, while quasars are inclined at small angles to the line of sight. However, the CSSs appear to be evolving in asymmetric environments. Comparison with larger sources and theoretical and numerical estimates of the symmetry parameters as the jets propagate outwards through such an asymmetric environment (Jeyakumar et al., in preparation) suggest that most sources may have passed through such a phase. These models yield ages for the CSSs in the range of $\sim 10^5 - 10^6$ yr, consistent with estimates from emission line studies (de Vries et al. 1999) and suggestions that the vast majority of CSSs are young sources (Fanti et al. 1995; Readhead et al. 1996a,b).

ACKNOWLEDGMENTS

We thank an anonymous referee for his valuable comments and suggestions. The Very Large Array is operated by the National Radio Astronomy Observatory for Associated Universities Inc. under a co-operative agreement with the National Science Foundation. The Arecibo Observatory is part of the National Astronomy and Ionosphere Center, which is operated by Cornell University under a cooperative agreement with the National Science Foundation. This research has made use of the NASA/IPAC extragalactic database (NED) which is operated by the Jet Propulsion Laboratory, Caltech, under contract with the National Aeronautics and Space Administration.

REFERENCES

- Antonucci R.R.J., 1993, ARA&A, 31, 473
- Baars J. W. M., Genzel R., Pauliny-Toth I. I. K., Witzel A., 1977, A&A, 61, 99
- Barthel P.D., 1989, ApJ, 336, 606
- Begelman M.C., 1996, In: Carilli C. L., Harris D. E. (eds.) Cygnus A - study of a radio galaxy. Proc. Greenbank Workshop, p. 209
- Carvalho J.C., 1985, MNRAS, 215, 463
- Dallacasa D., Fanti C., Fanti R., Schilizzi R.T., Spencer R.E., 1995, A&A, 295, 27
- Dallacasa D., Bondi M., Alef W., Mantovani F., 1998, A&AS, 129, 219
- de Vries W.H., O'Dea C.P., Baum S.A., Perlman E., Lehnert M.D., Barthel P.D., 1998, ApJ, 503, 156
- de Vries W.H., O'Dea C.P., Baum S.A., Barthel P.D., 1999, ApJ, 526, 27
- Dunlop J. S., Peacock J. A., Savage A., Lilly S. J., Heasley J. N., Simon A. J. B., 1989, MNRAS, 238, 1171
- Fanaroff B.L., Riley J.M., 1974, MNRAS, 167, 31P
- Fanti R., Fanti C., Schilizzi R.T., Spencer R.E., Nan Rendong, Parma P., van Breugel W.J.M., Venturi T., 1990, A&A, 231, 333
- Fanti C., Fanti R., Dallacasa D., Schilizzi R.T., Spencer R.E., Stangehelli C., 1995, A&A, 302, 317
- Hardcastle M.J., Alexander P., Pooley G.G., Riley J.M., 1998, MNRAS, 296, 445
- Henstock D. R., Browne I. W. A., Wilkinson P. N., Taylor G. B., Vermeulen R. C., Pearson T. J., Readhead A. C. S., 1995, ApJS, 100, 1

Junor W., Salter C.J., Saikia D.J., Mantovani F.M., Peck A.B., 1999, MNRAS, 308, 955

Kapahi V. K., 1981, A&AS, 43, 381

Kapahi V. K., Athreya R. M., Subrahmanya C. R., Baker J. C., Hunstead R. W., McCarthy P. J., van Breugel W., 1998a, ApJS, 118, 327

Kapahi V. K., Athreya R. M., van Breugel W., McCarthy P. J., Subrahmanya C. R., 1998b, ApJS, 118, 275

Laing R.A., Riley J.M., Longair M.S. 1983, MNRAS, 204, 151

Large M. I., Mills B. Y., Little A. G., Crawford D. F., Sutton J. M., 1981, MNRAS, 194, 693

Machalski J. & Condon J. J., 1983, AJ, 88, 143

Mantovani F., Junor W., Fanti R., Padrielli L., Saikia D.J., 1994, A&A, 292, 59

Mutel R.L., Phillips R.B., 1988, in Reid M.J., Moran J.M., eds, Proc. IAU Symp. 129, The impact of VLBI on Astrophysics and geophysics, Kluwer, p. 73

O'Dea C.P., 1998, PASP, 110, 493

Owsianik I., Conway J.E., 1998, A&A, 337, 69

Patnaik A. R., Browne I. W. A., Wilkinson P. N., Wrobel J. M. 1992, MNRAS, 254, 655

Pauliny-Toth I. I. K., Witzel A., Preuss E., Kühr H., Kellermann K. I., Fomalont E. B., 1978, AJ, 83, 451

Peacock J.A., Wall J.V., 1982, MNRAS, 198, 843

Readhead A.C.S., Taylor G.B., Xu W., Pearson T.J., Wilkinson P.N., Polatidis A.G., 1996a, ApJ, 460, 612

Readhead A.C.S., Taylor G.B., Pearson T.J., Wilkinson P.N., 1996b, ApJ, 460, 634

Saikia D.J., Kulkarni V.K., 1994, MNRAS, 270, 897

Saikia D. J., Jeyakumar S., Wiita P. J., Sanghera H. S., Spencer R. E., 1995, MNRAS, 276, 1215 (S95)

Sanghera H.S., Saikia D.J., Lüdke E., Spencer R.E., Foulsham P.A., Akujor C.E., Tzioumis A.K., 1995, A&A, 295, 629

Scheuer P.A.G., 1987, in Superluminal Radio Sources, eds, Zensus J.A., Pearson T.J., Cambridge Univ. Press, Cambridge, p. 104

Spencer R.E., McDowell J.C., Charlesworth M., Fanti C., Parma P., Peacock J.A., 1989, MNRAS, 240, 657

Stanghellini C., Baum S. A., O'Dea C. P., Morris G. B., 1990, A&A, 233, 379

Stanghellini C., O'Dea C. P., Baum S. A., Dallacasa D., Fanti R., Fanti C., 1997, A&A, 325, 943

Stickel M., Kühr H., 1994, A&AS, 103, 339

Taylor G. B., Vermeulen R. C., Readhead A. C. S., Pearson T. J., Henstock D. R., Wilkinson P. N., 1996, ApJS, 107, 37

Thakkar D. D., Xu W., Readhead A. C. S., Pearson T. J., Taylor G. B., Vermeulen R. C., Polatidis A. G., Wilkinson P. N., 1995, ApJS, 98, 33

Urry C. M., Padovani P., 1995, PASP, 107, 803

Wall J. V., Peacock J. A., 1985, MNRAS, 216, 173

Xu W., Readhead A. C. S., Pearson T. J., Polatidis A. G., Wilkinson P. N., 1995, ApJS, 99, 297